Electronic Supplementary Material (ESI) for Physical Chemistry Chemical Physics
This journal is © The Owner Societies 2013

Supplementary Information:

Can all nitrogen-doped defects improve the performance of graphene anode materials for lithium-ion batteries?

Yang-Xin Yu

Laboratory of Chemical Engineering Thermodynamics, Department of Chemical Engineering, Tsinghua University, Beijing 100084, People's Republic of China. E-mail: yangxyu@mail.tsinghua.edu.cn

1. Electronic density of state for the N-doped grapheme nanosheets

The electronic densities of state (DOS and PDOS) for the nine N-doped graphene nanosheets are listed in Figs. S1-S3. In Figs. S1 and S2, as well as Figs. S3e and S3f, the occupation numbers in the spin-up and spin-down states are equal, showing that the N_1, N_2^{AA}, N_2^{AB}, $N_2^{AB'}$, N_1V_1, pyridinic N_3V_1, and pyridinic N_4V_2 defects in graphene are nonmagnetic. However, from Figures S3a-d, we know that the pyrrolic N_3V_1 and pyridinic N_2V_2 are magnetic.

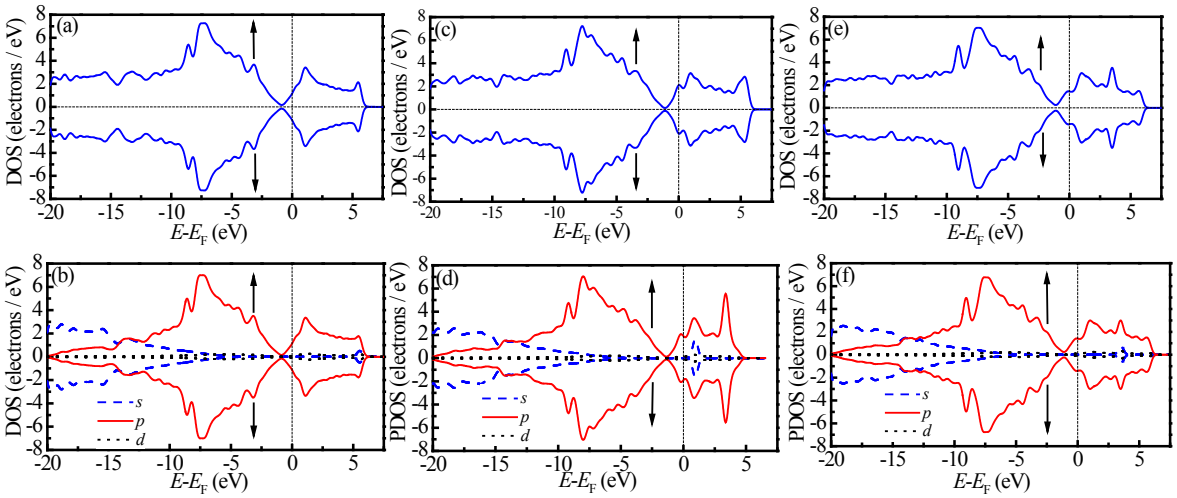

Fig. S1 (a) DOS for N_1, (b) PDOS for N_1, (c)DOS for N_2^{AA}, (d) PDOS for N_2^{AA}, (e) DOS for N_2^{AB} and (f) PDOS for N_2^{AB} conformations. The arrows denote spin-up (↑) and spin-down (↓) states.

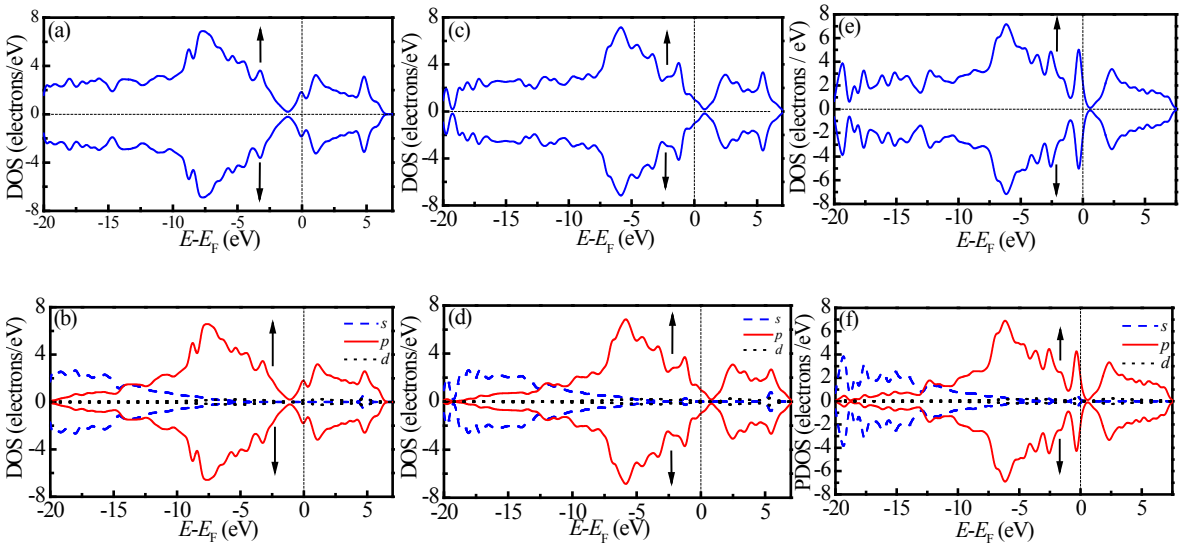

Fig. S2 (a) DOS for $N_2^{AB'}$, (b) PDOS for $N_2^{AB'}$, (c) DOS for N_1V_1, (d) PDOS for N_1V_1, (e) DOS for pyridinic N_3V_1, and (f) PDOS for pyridinic N_3V_1 conformations. The arrows have same meanings as in Figure S1.

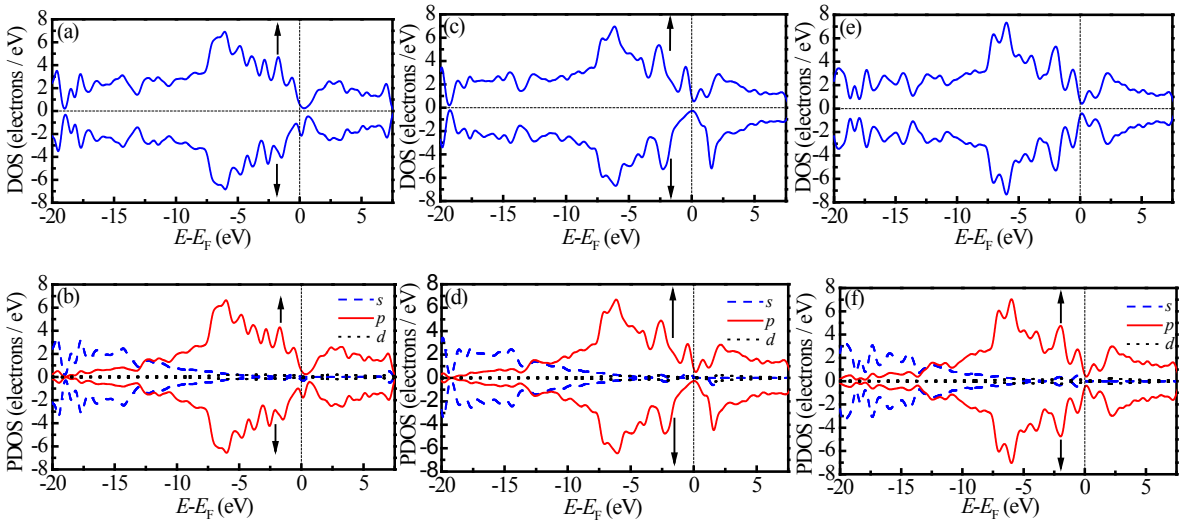

Fig. S3 (a) DOS for pyrrolic N_3V_1 , (c) DOS for pyridinic N_2V_2, (e) DOS for pyridinic N_4V_2. The arrows have same meanings as in Figure S1.

2. Magnetic moment variant in the optimization process for pyridinic-N_3V_1 defects

Evolutions of energy and magnetic moment in the process of optimization for pyridinic N_3V_1 defect in graphene are demonstrated in Fig. S4. From Figure S4 one can see that the stable structure of the pyridinic N_3V_1 defect in graphene is nonmagnetic state. Both methods (DMol^3 and CASTEP) predict that the magnetic state for the pyridinic N_3V_1 defect in graphene is unstable. In the CASTEP calculation, the ultrasoft pseudopotentials generated with the atomic valence configurations of C($2s^22p^2$) and N($2s^22p^3$)

were used and the vdW dispersion correction was included in the density functional theory calculations.

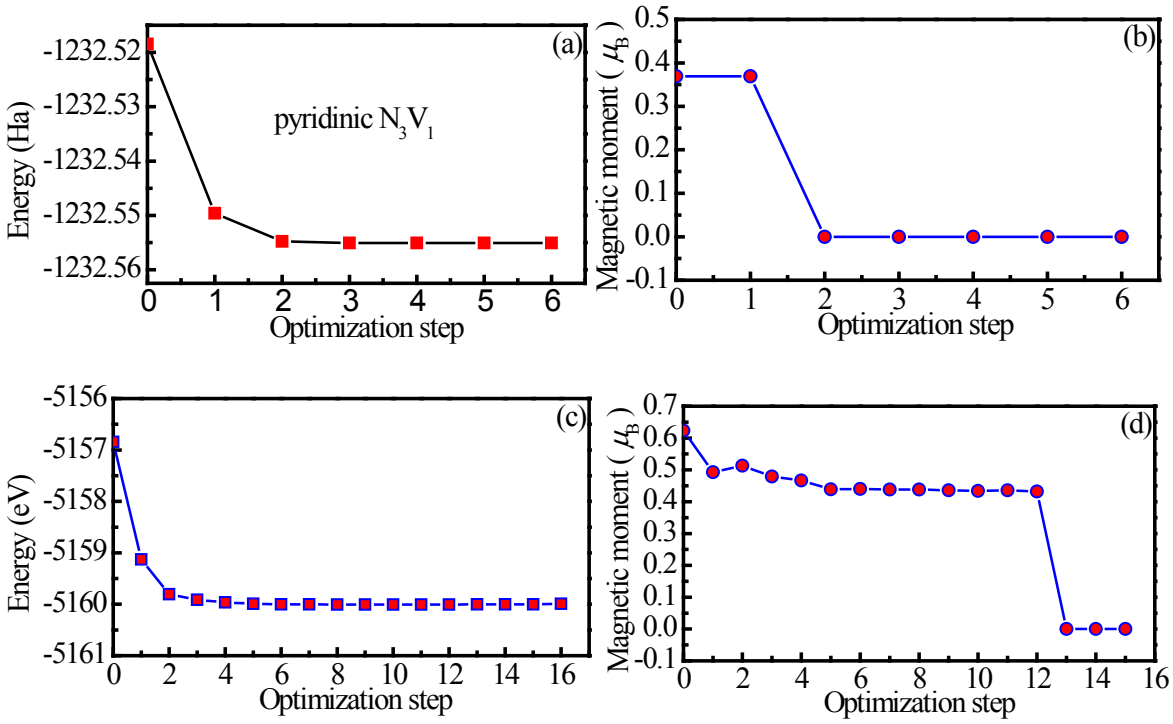

Fig. S4 Evolutions of energy and magnetic moment in the process of optimization for pyridinic N_3V_1 defect: (a) energy from DMol^3, (b) magnetic moment from DMol^3, (c) energy from CASTEP and (d) magnetic moment from CASTEP.

3. Formation energy of lithium adsorbed on N-doped graphene

The optimized stable structures, formation energies and the heights of lithium atom from the base plane of graphene for the N1, N_2^{AA}, N_2^{AB} and $N_2^{AB'}$ configurations are presented in Figs. S5-S8, respectively.

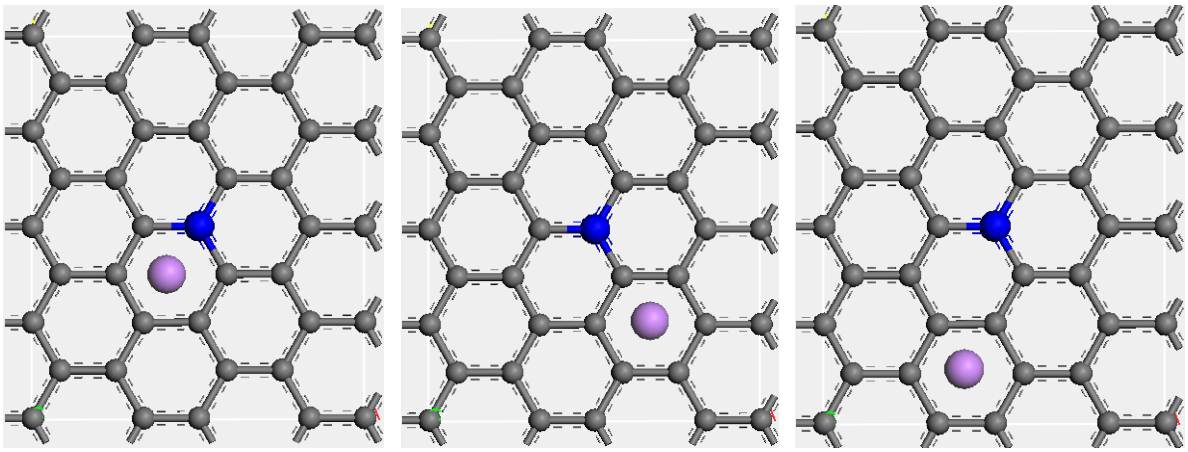

(a) $\triangle E_f$ = 2.89 eV, h = 2.89 Å (b) $\triangle E_f$ = 2.67 eV, h = 2.71 Å (c) $\triangle E_f$ = 2.62 eV, h = 1.70 Å

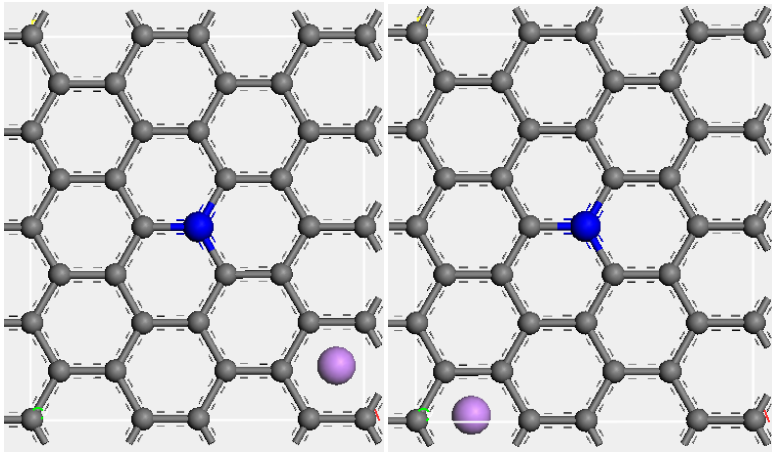

(d) $\triangle E_f$ = 2.61 eV, h = 1.69 Å (e) $\triangle E_f$ = 2.57 eV, h = 1.68 Å

Fig. S5 Geometries, formation energies and heights of lithium atom to the base plane of graphene for different adsorption sites on the N_1 defect at 0 K. The small gray, middle-sized blue and large pink balls represent carbon, nitrogen and lithium atoms, respectively.

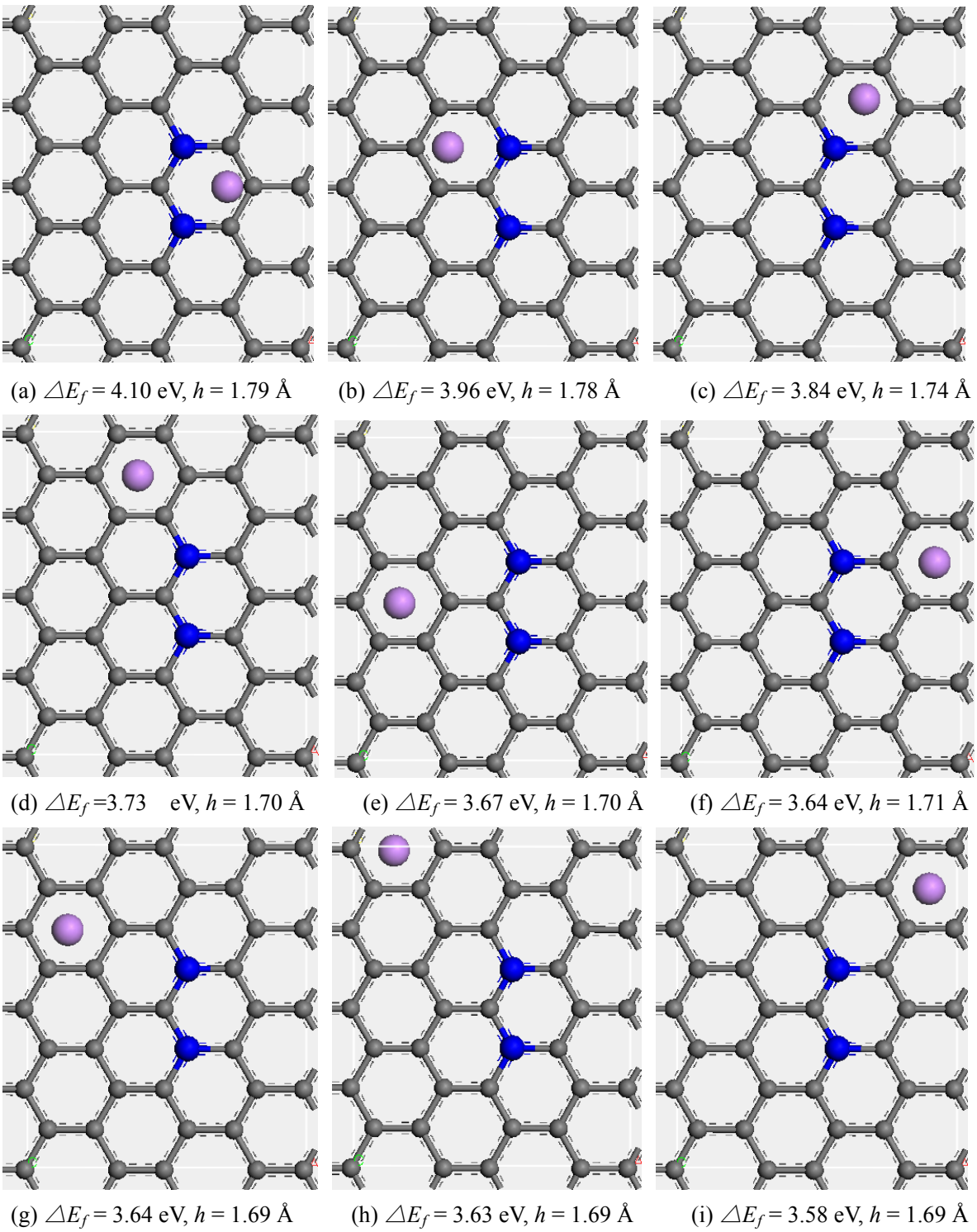

Fig. S6 Optimized geometries, formation energies and adsorption heights of one lithium atom on different sites of the N_2^{AA} defect at 0 K. The small gray, middle-sized blue and large pink balls represent carbon, nitrogen and lithium atoms, respectively.

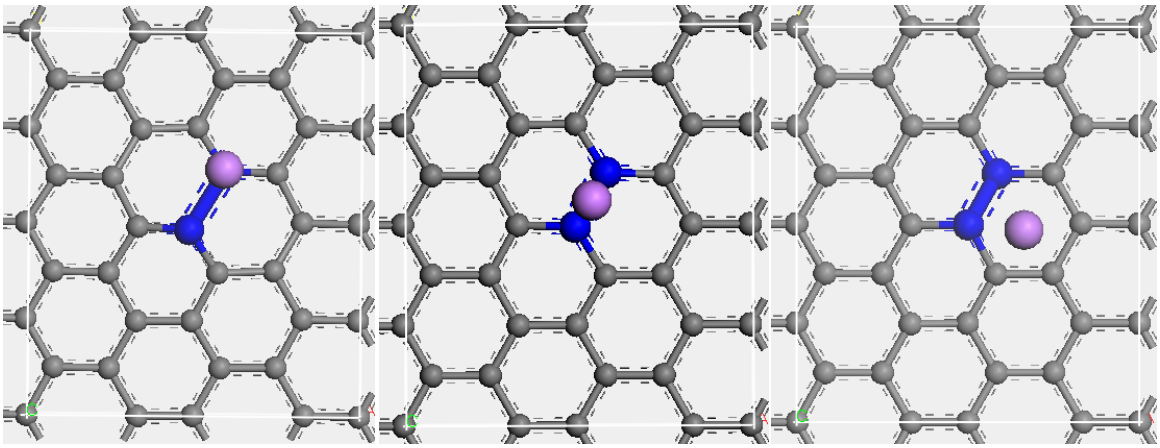

(a) $\triangle E_f$ = 3.40 eV, h = 1.42 Å (b) $\triangle E_f$ = 4.81 eV, h = 1.78 Å (c) $\triangle E_f$ = 4.35 eV, h = 1.83 Å

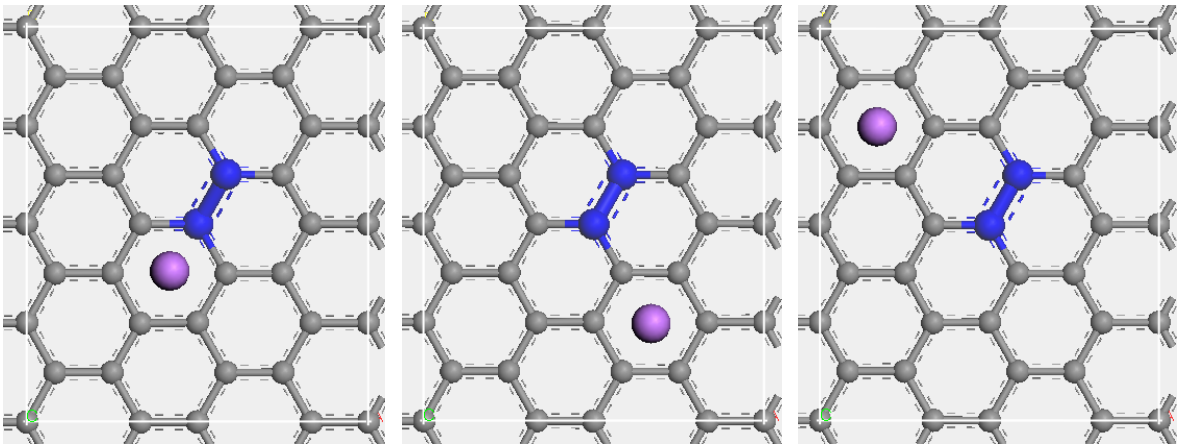

(d) $\triangle E_f$ = 4.46 eV, h = 1.83 Å (e) $\triangle E_f$ = 4.39 eV, h = 1.70 Å (f) $\triangle E_f$ = 4.37 eV, h = 1.68 Å

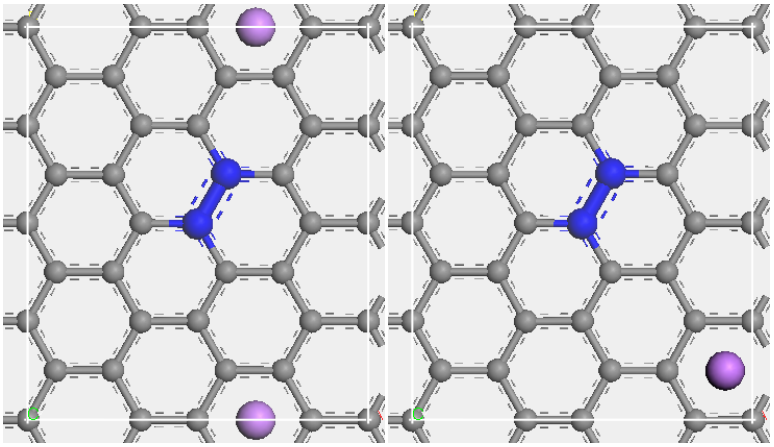

(g) $\triangle E_f$ = 4.42 eV, h = 1.69 Å (h) $\triangle E_f$ = 4.34 eV, h = 1.68 Å

Fig. S7 Optimized geometries, formation energies and adsorption heights of one lithium atom on different sites of the N_2^{AB} defect at 0K. The small gray, middle-sized blue and large pink balls represent carbon, nitrogen and lithium atoms, respectively.

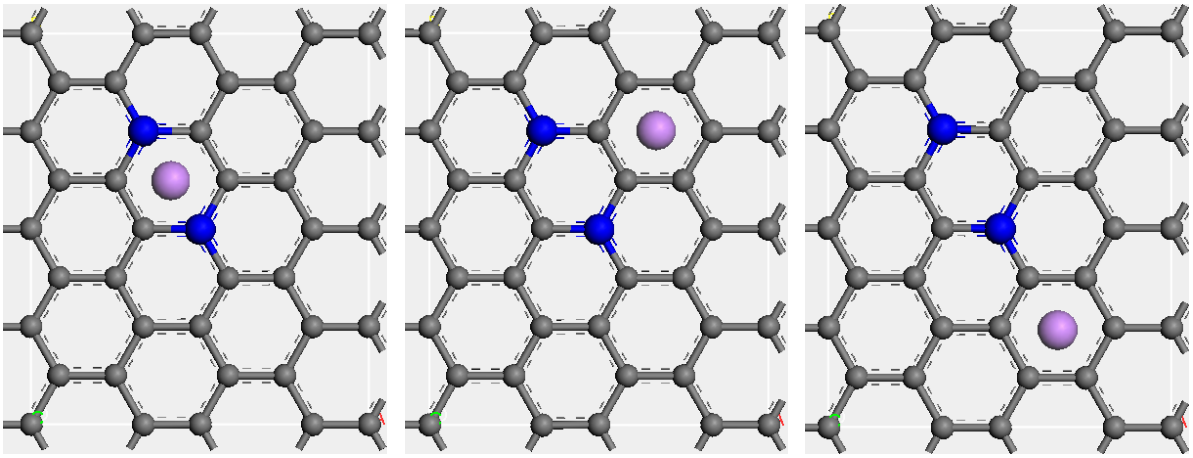

(a) $\triangle E_f$ = 3.74 eV, h = 1.77 Å (b) $\triangle E_f$ = 3.38 eV, h = 1.72 Å (c) $\triangle E_f$ = 3.32 eV, h = 1.70 Å

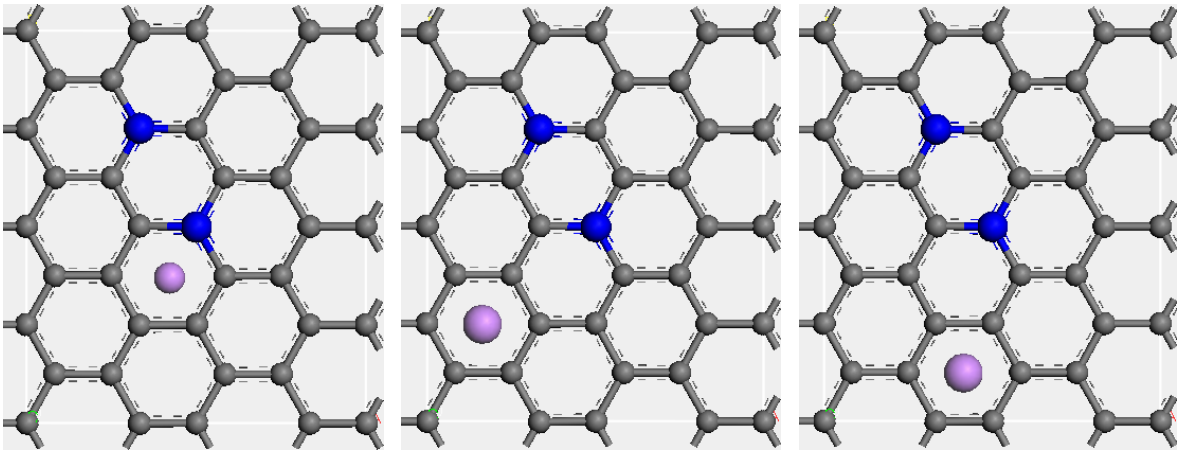

(d) $\triangle E_f$ = 3.52 eV, h = 1.73 Å (e) $\triangle E_f = 3.32_{-1}$ eV, h = 1.68 Å (f) $\triangle E_f = 3.31_{+3}$ eV, h = 1.69 Å

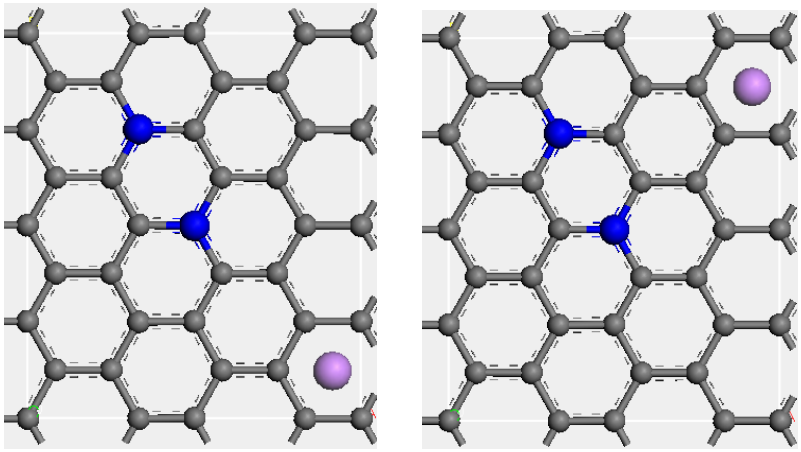

(g) $\triangle E_f = 3.31_{-0.2}$ eV, h = 1.68 Å (h) $\triangle E_f$ = 3.30 eV, h = 1.70 Å

Fig. S8 Optimized geometries, formation energies and adsorption heights of one lithium atom on different sites of the $N_2^{AB'}$ defect at 0K. The small gray, middle-sized blue and large pink balls represent carbon, nitrogen and lithium atoms, respectively.